NTNU
Norwegian University of Science and Technology

Department of Chemical Engineering

TKP4580 - Chemical Engineering, Specialization Project

Open Loop Dynamic Optimization of Aluminium Extrusion

Author:
Mats Kulås

Supervisors:
Johannes Jäschke
Anne Øyen Halås

December 16, 2021

Abstract

Aluminium is used in many applications today, like in large scale construction, carabiners for climbing and car parts. Some of the uses, like radiators in cars, benefit from using very thin aluminium profiles. These profiles are made using a process called extrusion. Here, a cylinder of aluminium is heated up and pressed through a smaller hole determining the cross-sectional shape of the extruded profile. The tool containing this hole is called the die, and the cylinder is usually referred to as a billet. A problem in creating thin profiles using this process is that they are subject to deformation and tearing if the temperature during extrusion is not controlled well. To be able to reduce the thickness, better temperature control therefore needs to be developed.

In this project, the application of open loop dynamic optimization to improve the operation of extrusion presses for aluminium was studied. The goal was to optimize the initial temperature of the aluminium before extrusion, as well as the ram speed of the extrusion press, to achieve good set point tracking for the temperature inside the die shaping the extruded profile and minimizing the extrusion time. An existing first principle model based on finite differences was used to describe the process. Optimization problems using the initial temperature of the billet and the ram speed as inputs were formulated, and they were solved using Cybernetica CENIT.

The results showed that very good set point tracking for the temperature was possible. When only the initial temperature was optimized and the ram speed was fixed, deviations up to 5 °C from the set point were observed, but when ram speed also was included as an input no significant deviations were observed. A comparison with data for an extrusion cycle from Hydro showed that variations in the temperature were significantly reduced by the optimization. A significant reduction in the extrusion time was also accomplished, without making the set point tracking worse. Based on these results, dynamic optimization seems a promising way to improve operation of extrusion presses. Further work on this problem should consider including the pre-heater of the billet in the optimization problem, as well as including the cooling capabilities of the extrusion press.

Contents

1 Introduction

1.1 Background

Aluminium is among the most commonly used metals today, due to its low weight and high strength. It is also cheap to recycle, and it can be infinitely recycled. These properties make it a very desirable material as the focus on sustainability increases, and it is used in a wide variety of applications. For example, aluminium is used to make parts for cars and in construction, as well as everyday objects like phones and computers [9]. In cars, one common usage is in the radiator. Here, thin walled aluminium profiles as shown in Figure 1.1 are used for heat transfer. To reduce their weight and increase heat transfer it is desirable to make them as thin as possible. They are produced by a process called extrusion, and when the profiles get very thin they are subject to tearing and deformation if the temperature during extrusion varies too much. To make them thinner, precise temperature control of the extruded aluminium is therefore important. To increase the efficiency of the process, performing the extrusion as fast as possible is also desirable. This would increase the productivity of the extrusion presses, which would result in higher profitability for the process. The goal of this project is therefore to improve the temperature control of the extruded aluminium while also minimizing the extrusion time using open loop dynamic optimization.

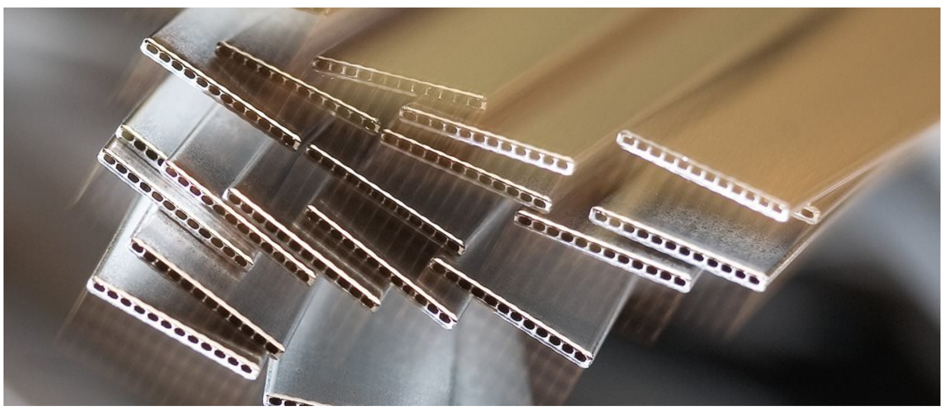

Figure 1.1: Picture of thin walled micro channel tubes from Hydro [12]

This project is part of the larger ExtruTeC project, which is a collaboration between Cybernetica, Hydro, SINTEF and NTNU [14]. The goal of ExtruTeC is to develop both a system for batch optimisation for the extrusion cycle and model predictive control for the temperature. In this project the batch optimization will be considered. An existing model of the extrusion press made by Cybernetica will be used for the open loop dynamic optimization.

1.2 Literature review

Several studies have been performed on the modelling and optimization of aluminium extrusion previously. Mostly, finite element simulations have been used and optimization has been performed to keep the peak temperature of the extruded aluminium close to a desired set point. Below follows a brief overview of previous work in the field.

Matamoros [7] developed a semi-analytical model for the extrusion process, where equations of motions and continuity were solved analytically while the energy balance was solved using finite elements. This significantly reduced the computation time needed for simulations compared to approaches only using finite elements, and comparisons with data from industry showed that the model described the process well. Strategies for temperature control also examined, as well as implementation of nonlinear model predictive control for the process. Simulations showed that good temperature control could be achieved by manipulating the extrusion speed, but this was not validated on a real extrusion press. The simulations were performed using an initial predefined linear temperature gradient for the aluminium billet.

Bastani et al.[2] used finite element simulations to investigate isothermal extrusion of aluminium. They studied the effect of the initial front temperature of the billet, the initial temperature gradient, ram speed and cooling rate in the container on the exit temperature of the extruded aluminium. They found that for low initial temperature gradients the exit temperature could be kept close to constant using a constant ram speed. For higher initial gradients the ram speed must be varied during the extrusion cycle to keep the temperature constant.

Bastani et al.[3] used both a 3D and 2D finite element model to simulate aluminium extrusion with varying ram speeds, initial temperatures of the billet and cooling rates, with the aim of finding parameters which would minimize radial variations in temperature and flow velocity as well as obtaining isothermal extrusion. They showed that the difference between the 2D and 3D model was small, and that the initial temperature taper of the billet had a significant effect on how much the exit temperature of the extruded aluminium varied. As in Bastani et al.[2] they also found that isothermal extrusion was easiest to obtain with low tapers in the billet, and that non-constant ram speed must be used to achieve isothermal extrusion for higher tapers.

1.3 Scope of the project

This project aims to study the viability of using open loop dynamic optimization on extrusion of aluminium. The model of the process provided by Cybernetica is still under development, and calculated values may therefore not accurately describe the behaviour of the real system. Nevertheless, the model was assumed accurate enough to study whether utilization of dynamic optimization on an extrusion press can improve operation. The project was undertaken as part of the specialization course TKP4580 at the Department of Chemical Engineering at NTNU. It gives 15 student credits, which corresponds to half the work load of a semester.

This report will first give an introduction to the extrusion process. Then, the model used in the optimization will be described. The optimization problem is then described, and the results from different approaches and formulations are described and compared.

2 System Description

2.1 Extrusion

Extrusion is a process of deforming materials like metals, polymers and concrete into straight profiles with a constant cross-sectional shape. There exist several different methods of extrusion, the most common of which are direct and indirect extrusion. In direct extrusion a ram is used to press a cylindrical billet through a die, which is a hole determining the shape of the extruded profile. Indirect extrusion uses a hollow ram, and instead of pushing the material through a die at the end of the container it flows back through the ram. These methods are illustrated in Figures 2.1 and 2.2. The main difference between them is that there is much less friction in indirect extrusion, as the billet does not move relative to the container. This means less heat is generated and less force from the ram is needed[7]. The most common method today is direct extrusion, and it is also used by Hydro in the process studied in this project. Therefore, only direct extrusion will be considered in the rest of this report.

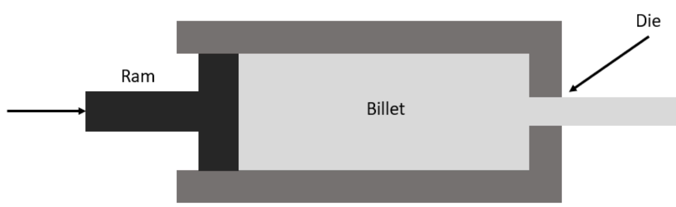

Figure 2.1: Simple illustration of direct extrusion

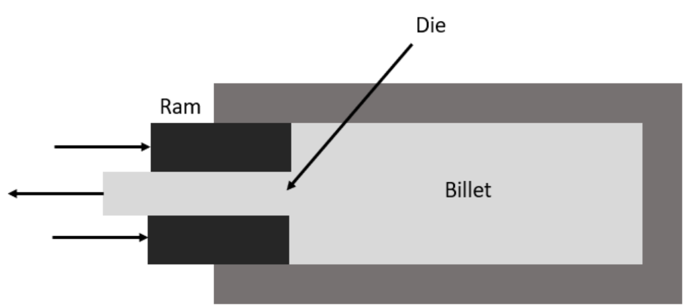

Figure 2.2: Simple illustration of indirect extrusion

Extrusion is a common way to treat aluminium. The quality of the extruded aluminium is highly dependent on the highest temperature in the die during extrusion, here referred to as the peak temperature T_{peak}. Due to heat generation from friction, deformation etc. it is difficult to control, and to counteract the heat generation in the billet during the extrusion cycle two methods are commonly used. One is to generate an initial temperature profile on the billet. Frictional forces cause the billet to increase in temperature towards the end of the extrusion cycle, so the front part, which is extruded first, is heated to be warmer than the back part. This is usually done in a gas furnace or induction heater. The aim is therefore to have a large enough temperature gradient in the billet to counteract the heat generating forces during the extrusion cycle, resulting in a constant peak temperature for the extruded aluminium. Usually linear temperature profiles, often called tapers, are used in industry today, and the extrusion is usually performed with constant ram speed[3].

The other method is to adjust the ram speed. Heat generation is highly dependent on how fast the extrusion is performed, and increasing or reducing the ram speed during the press cycle can help keep the peak temperature in the die constant. If this method is used the extrusion can be performed with constant initial temperature and a decreasing ram speed. Combinations of the two methods can also be used. An initial taper can be induced on the billet, and ram speed can be adjusted based on measurements or follow a predetermined program to keep the peak temperature constant [7].

2.2 Hydro Extruded Solutions - Precision Tubing

This project concerns one of Hydros extrusion processes, and it will therefore be described in more detail. It is run by Hydro Extruded Solutions - Precision Tubing, and produces thin walled MultiPort Extrusions (MPE), which means there are several holes in the die. An illustration is shown in Figure 2.3. The process is based on direct extrusion, with billets of length 0.9 m and diameters of 0.2286 m. Before the billet is loaded into the press, it is heated in an induction heater using 4 or 6 heating points depending on billet length. Using this heater a linear taper is created, and the extrusion is then performed with a constant ram speed. To achieve good product quality, the temperature T_{peak} shown in Figure 2.3 should be kept close to a desired set point dependent on the alloy being extruded. Today, this is achieved through manipulating the initial taper, ram speed and cooling in the die based on recipes for each product and operator experience. The resulting T_{peak} and ram speed for an extrusion cycle at one of Hydro's presses can be seen in Figure 5.1. The corresponding initial taper is shown in Figure 5.2. In this extrusion no cooling was used.

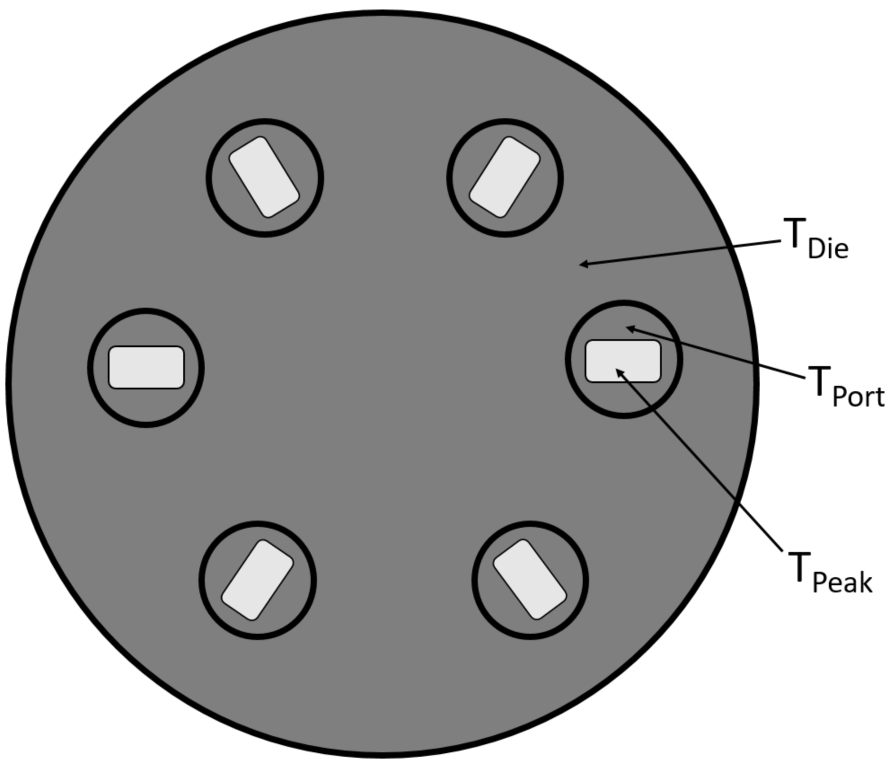

Figure 2.3: Illustration of the die used in the extrusion process. The light grey areas are the ports the aluminium passes through during extrusion. T_{Die}, T_{Port} and T_{Peak} are important temperatures in the model. T_{Peak} is located further down inside the hole than T_{Port}, where the aluminium is formed into its desired shape.

The products from this process are thin walled, flat structures with hollow inner channels as shown in Figure 2.4. They are intended for use in heat exchangers and are therefore desired to be thin, to increase heat transfer and reduce aluminium usage. The exact dimensions are confidential information, but the thicknesses are less than a millimetre and height and width are of orders of magnitude millimetres and centimetres respectively.

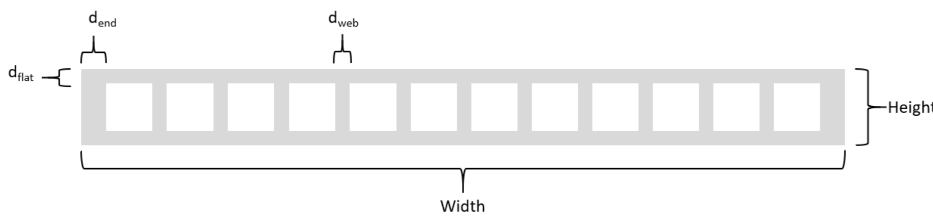

Figure 2.4: Illustration of the cross section of an extruded profile. d_{end}, d_{flat} and d_{web} are the thicknesses of the end walls, the top/bottom walls and the inner walls of the profile respectively.

3 Model Description

The model of the extrusion press used was made by Cybernetica, and its development was not a part of this project. It was however used in the optimization, and a brief description of its structure is therefore included. The billet was modelled using a cylindrical coordinate system, with the coordinates shown in Figure 3.1.

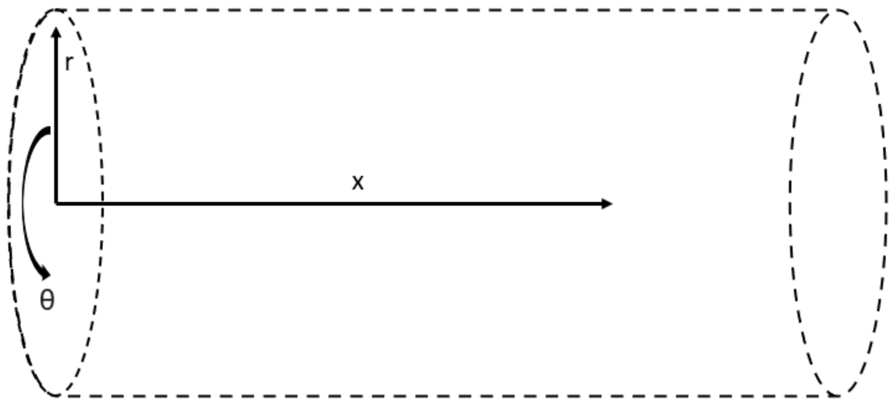

Figure 3.1: Illustration of the coordinate system used for the model.

The temperature in the billet is calculated using the equation of energy in cylindrical coordinates [4]:

$$\begin{aligned}\rho\hat{C}_p\left(\frac{\partial T}{\partial t}+v_r\frac{\partial T}{\partial r}+\frac{v_\theta}{r}\frac{\partial T}{\partial \theta}+v_x\frac{\partial T}{\partial x}\right)=&-\left[\frac{1}{r}\frac{\partial}{\partial r}(rq_r)+\frac{1}{r}\frac{\partial q_\theta}{\partial \theta}+\frac{\partial q_x}{\partial x}\right]\\&-\left(\frac{\partial \ln\rho}{\partial \ln T}\right)_p\frac{Dp}{Dt}-(\boldsymbol{\tau}:\boldsymbol{\nabla}\boldsymbol{v})\end{aligned}\tag{3.1}$$

Here, ρ is the density, $\hat{C}_p$ is the heat capacity, T is the absolute temperature and t is time. v and q are velocity and conductive heat flux in the direction marked in the subscript and p describes the pressure. The term $-(\boldsymbol{\tau}:\boldsymbol{\nabla}\boldsymbol{v})$ is viscous dissipation, which describes how mechanical energy in the flow degrades into thermal energy. The products of v_i and derivatives of T by i, where $i=x,r,\theta$, are convection terms and the terms inside square brackets on the right side describe conduction [4]. The equation is simplified using the following assumptions:

- Symmetry around the x-axis $\Rightarrow$ All derivatives of θ are zero
- Only flow in the x-direction $\Rightarrow$ v_r and v_θ are zero
- The aluminium flow can be described as a non-Newtonian incompressible fluid $\Rightarrow$ ρ constant

The simplified equation thus becomes

$$\rho\hat{C}_p\left(\frac{\partial T}{\partial t}+v_x\frac{\partial T}{\partial x}\right)=-\left[\frac{1}{r}\frac{\partial}{\partial r}(rq_r)+\frac{\partial q_x}{\partial x}\right]-\left(-\mu\left(\frac{\partial v_x}{\partial r}\right)^2\right)\tag{3.2}$$

where the last term is the simplified term for viscous dissipation. As the flow is assumed non-Newtonian the viscosity μ is not constant, but instead a function of the effective strain rate and effective deviatoric stress [1]. Fourier's law [6] can be used to express the remaining conductive heat fluxes:

$$q_x = -k_{\mathrm{Al}} \frac{\partial T}{\partial x} \tag{3.3}$$

$$q_r = -k_{\mathrm{Al}} \frac{\partial T}{\partial r} \tag{3.4}$$

where k_{Al} is the thermal conductivity of the aluminium alloy. This yields the following equation for calculating $\frac{\partial T}{\partial t}$:

$$\frac{\partial T}{\partial t} = -v_x \frac{\partial T}{\partial x} + \alpha \left[\frac{1}{r} \frac{\partial}{\partial r} \left(r \frac{\partial T}{\partial r} \right) + \frac{\partial^2 T}{\partial x^2} \right] + \frac{\mu}{\rho \hat{C}_p} \left(\frac{\partial v_x}{\partial r} \right)^2 \tag{3.5}$$

where α is the thermal diffusivity given by the formula

$$\alpha = \frac{k_{\mathrm{Al}}}{\rho \hat{C}_p} \tag{3.6}$$

Equation 3.5 is solved using finite differences [11], which means using the approximations

$$\frac{\partial T}{\partial t}(i,j,k) \approx \frac{T(i,j,k+1) - T(i,j,k)}{\Delta t} \tag{3.7}$$

$$\frac{\partial T}{\partial x}(i,j,k) \approx \frac{T(i+1,j,k) - T(i,j,k)}{\Delta x} \tag{3.8}$$

$$\frac{\partial T}{\partial r}(i,j,k) \approx \frac{T(i,j+1,k) - T(i,j-1,k)}{2\Delta r} \tag{3.9}$$

$$\frac{\partial^2 T}{\partial x^2}(i,j,k) \approx \frac{T(i+1,j,k) - 2T(i,j,k) + T(i-1,j,k)}{\Delta x^2} \tag{3.10}$$

$$\frac{\partial^2 T}{\partial r^2}(i,j,k) \approx \frac{T(i,j+1,k) - 2T(i,j,k) + T(i,j-1,k)}{\Delta r^2} \tag{3.11}$$

Here, i marks the placement of the point in the x-direction, j the placement in the r-direction and k marks the time step. For the approximation of the first derivative of T by r and both second derivatives central differences were used. For the others, forward differences were used. The grid for the billet is made of 18 points in the x-direction and 6 in the r-direction, and an illustration of the grid structure is shown in Figure 3.2.

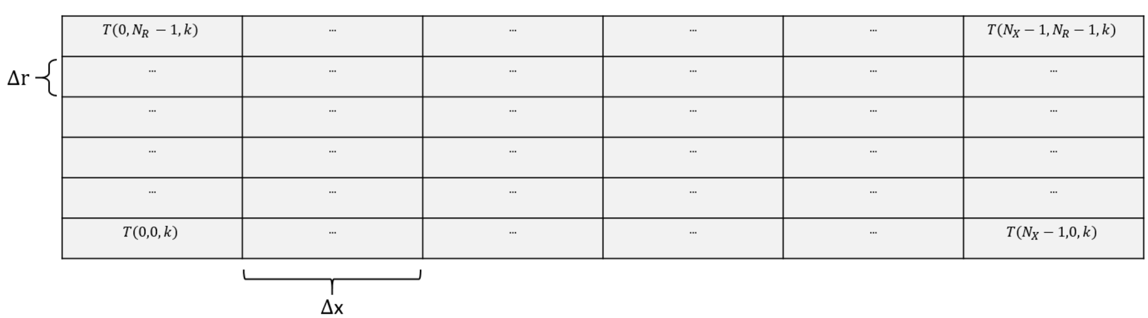

Figure 3.2: Illustration of the grid structure used to model the billet. N_X equals 18 and N_R equals 6. Δx and Δr are the distances between the points in the axial and radial direction.

As the extrusion cycle progresses, the ram passes through the points in the grid starting at the points where x equals $N_X - 1$. The derivatives of all states in these points are then set to zero, as there is no more billet left in these points in the grid. As the billet is being extruded it passes through several stages of reduction in its cross sectional area. First it passes into the feeding zone, a section where the cross sectional area of the aluminium is reduced. Then it goes to the port, where the aluminium is fed into the die. Then it is shaped into the desired final profile. Here, in the final shaping it reaches its highest temperature T_{peak}. This grid structure is shown in Figure 3.3.

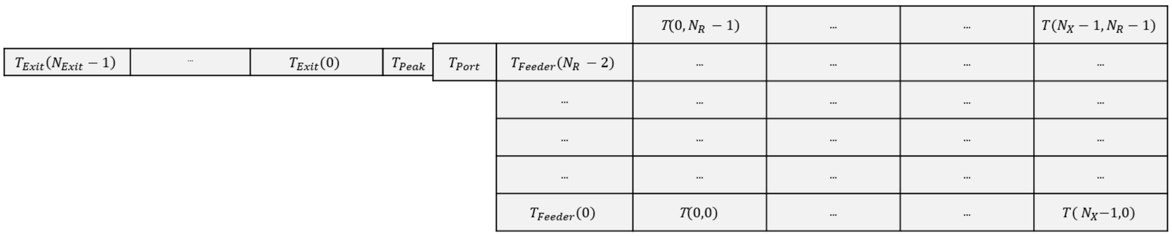

Figure 3.3: Illustration of the grid structure used to model the entire extrusion process.

At each reduction of area the assumption of incompressible flow is used to calculated the new velocity of the flow from the mass balance over the reduction zone:

$$v_2 = \frac{A_1}{A_2} v_1 \tag{3.12}$$

Here, v_2 and A_2 are the velocity and cross sectional area out of the shrinking section, while v_1 and A_1 are for the inflow. In addition, heat generation due to the reduction in area is added, but these equations are classified and thus cannot be disclosed here. They are however based on the same material model. The control volumes for T_{peak} and T_{port} are small compared to the others, and a quasi steady state assumption is therefore made on these volumes to avoid numerical problems caused by stiff systems [13]. This means assuming that since these control volumes are much smaller than the others, their dynamics are much faster. Therefore, they can be assumed to change "instantaneously" compared to the other control volumes, which means they are both directly calculated from the temperature in the feeder. The model was implemented in Cybernetica Model and Application Component, described in Section 4.5.

The model has been compared to temperature measurements by Hydro. T_{port} and T_{die} were measured, and a plot comparing them to values calculated by the model is shown in Figure 3.4. It shows that the model captures the behaviour of the system well, even though there are some deviations from the measurements for T_{die}. The value of T_{peak} is not measured by Hydro, so comparisons to the model cannot be made. However, it is assumed that since T_{port} and T_{die} are described well by the model T_{peak} will also be described well.

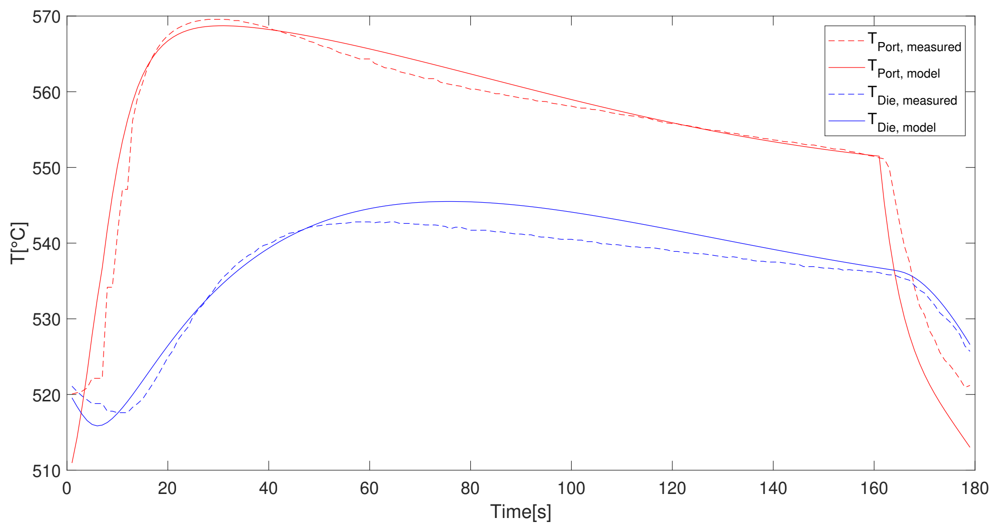

Figure 3.4: Comparison of measured data for T_{port} and T_{die} to calculated values. Data provided by Cybernetica.

4 Dynamic Optimization

An optimization problem is a mathematical problem where the goal is to minimize or maximize the value of a scalar function $f(x)$, called the objective function. This is done by adjusting the values in the vector x, which are called the inputs or variables. These are often subject to constraints, which can be both equality and inequality constraints. They are often described with the letters c and g[8]. The formulation of the problem then becomes

$$\begin{aligned} \min_{x} \; & f(x) \\ \text{s.t.} \; & g(x) \leq 0 \\ & c(x) = 0 \end{aligned} \tag{4.1}$$

This can be illustrated with a simple example. Consider the objective function $f(x) = x_1^2 + x_2^2$ with the constraint $c(x) = (x_1 - 3)^2 - 2x_2 \leq 0$. The optimization problem can be formulated as

$$\begin{aligned} \min_{x_1, x_2} \; & x_1^2 + x_2^2 \\ \text{s.t.} \; & (x_1 - 3)^2 - 2x_2 \leq 0 \end{aligned} \tag{4.2}$$

A plot of the problem is shown in Figure 4.1. The feasible region, where the constraints are satisfied, is above the line marked $c(x)$, and the solution to the problem is the point closest to the point $x = (0, 0)$, where $f(x)$ has its unconstrained minimum.

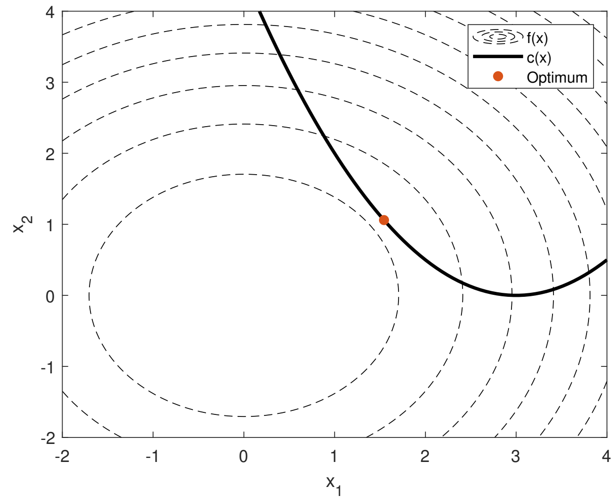

Figure 4.1: Plot of the optimization problem in Equation 4.2.

In dynamic optimization the goal is to find the optimal behaviour of a system by solving an optimization problem where a dynamic model of the system is included in the constraints [5]. For discrete time models they can be written on the form

$$\begin{aligned}
\min_{u} \quad & \sum_{t=0}^{N-1} J(x_{t+1}, u_t) \\
\text{s.t.} \quad & x_{t+1} = g(x_t, u_t) \\
& c(x_t, u_t) \leq 0 \\
& x_{min} \leq x_t \leq x_{max} \\
& u_{min} \leq u_t \leq u_{max} \\
& -\Delta u_{max} \leq \Delta u_t \leq \Delta u_{max} \\
& x_0, u_{-1} = \text{given}
\end{aligned} \tag{4.3}$$

Here, x describes the states in the system and u the input variables. The inputs can be adjusted to minimize the objective function J, which is used to define what is considered the optimal behaviour for the system. It is a scalar function which can describe costs, energy usage of a process, deviations of states from set points or other relevant values. $g(x, u)$ is the discrete dynamic model of the process and $c(x, u)$ describes path constraints for the process. The inequality constraints on x can describe physical constraints on the states, like for example non-negative pressures or mass. The inequality constraints on u and Δu can describe physical limitations in inputs on how fast they can be changed, like for example maximum and minimum valve positions.

In this project dynamic optimization of an extrusion press was considered. The objective was to keep the maximum temperature of the aluminium during extrusion at a desired set point. The aluminium is warmest as it passes through the thinnest passage in the die, and the temperature here is called T_{peak}. The second objective was to perform the extrusion as fast as possible while still fulfilling the first objective, to increase the productivity of the extrusion press. In the first part of the project the initial temperature profile of the billet, the taper, was used as the input for the optimization problem, and only the first objective was considered. This is described in Section 4.2. In the second part the taper found in part one was used as the initial condition for optimization using the ram speed of the press as the input, again only considering the objective of keeping T_{peak} close to its set point.

This is described in Section 4.3. In the last part both the initial taper and ram speed were used as inputs simultaneously, and both objectives were considered. This is described in Section 4.4.

4.1 Constraints

Both the initial taper of the billet and the ram speed are subject to constraints. Hydro operates with a minimum temperature gradient of 40 °C/m, with the warmest end being the one extruded first, referred to as the front end in this report. This is because higher temperatures makes the deformation of aluminium easier. If parts of the billet further back are warmer than in front this can result in undesirable flow patterns during extrusion, reducing product quality. The reason the minimum gradient is so high is that the temperature control in the heater used to induce the initial taper is imprecise, as it only has 6 heating points. This means local temperature variations in the billet can cause flow problems if the gradient is not high enough. Hydro also only use linear tapers for the billets. As this project is part of a larger project to improve control of the extrusion process, test were also performed to see how better temperature control in the heaters could improve the process. Optimization was therefore also performed with a minimum temperature gradient of 10 °C/m, without the constraint of a linear temperature profile. For both cases the initial temperature was considered uniform in the radial direction.

The ram speed is usually operated at 4 mm/s, but the maximum possible speed is assumed to be 5 mm/s. The maximum acceleration of the ram is also assumed to be constrained to 0.4 mm/s^2.

4.2 Optimizing using initial temperature profile

Here, the inputs in the optimization problem was the initial temperature profile of the billet before extrusion, and the ram speed was considered fixed to a given speed profile. It consisted of a constant acceleration of 0.4 mm/s^2 for 10 s, and then a constant speed of 4 mm/s for the rest of the extrusion cycle. Two different formulations of the optimization problem were considered, one which followed Hydro's constraint of a linear profile with a minimum gradient of 40 °C/m and one which followed the more relaxed constraint of minimum 10 °C/m without having to be linear. For both cases constraints were added to the value of T_{peak}. The upper constraint was 2 °C above the set point, while the lower constraint was 5 °C below. This was because temperature variations above the set point are expected to have a larger negative effect on product quality the variations below, so tighter constraints were needed.

For the case with Hydro's constraints only the temperatures at the front and back of the billet were used as inputs in the optimization problem, and the rest of the temperatures were calculated by linear interpolation. The optimization problem therefore had two inputs, and could be formulated as

$$
\begin{aligned}
\min_{u_{\text{T,init}}} \quad & \sum_{t=0}^{N-1} (T_{\text{peak, t+1}} - T_{\text{peak, sp}})^2 + \rho\epsilon_{t+1} \\
\text{s.t.} \quad & x_{t+1} = g(x_t, u_{\text{T,init}}) \\
& c(x_t, u_{\text{T,init}}) \leq 0 \\
& x_{min} \leq x_t \leq x_{max} \\
& T_{\text{peak, sp}} - 5\,^\circ\text{C} - \epsilon_t \leq T_{\text{peak, t}} \leq T_{\text{peak, sp}} + 2\,^\circ\text{C} + \epsilon_t \\
& \epsilon_t \geq 0 \\
& 0\,^\circ\text{C} \leq u_{\text{T,init}} \leq 660\,^\circ\text{C} \\
& T_{\text{front}} - T_{\text{back}} \geq 36\,^\circ\text{C} \\
& T_{\text{peak, 0}} = 520\,^\circ\text{C}
\end{aligned}
\tag{4.4}
$$

Here, $u_{\text{T,init}}$ was equal to the vector $[T_{\text{front}}, T_{\text{back}}]$. The constraints on T_{peak} were added as soft constraints to the objective function, to avoid infeasible solutions. The value of ϵ_t will become nonzero if the constraint is violated, giving a large increase in the objective function as ρ is a large positive scalar value. The upper and lower bounds on the inputs describe the absolute limits on the temperature region for extrusion of aluminium. It cannot be below the freezing point, and it cannot be above the melting point of aluminium[9]. The constraint on the minimum difference between T_{front} and T_{back} comes from the minimum gradient constraint, and that the billet considered was 0.9 m long. The initial condition on T_{peak} comes from the fact that the die cools between each extrusion and conductive heat transfer to already extruded aluminium, which is in contact with air. This reduces the temperature of the aluminium extruded first in every cycle. The exact value is dependent on the temperatures during the last extrusion cycle and the time between extrusion, and is therefore difficult to know precisely. 520 °C was however assumed to be a good estimate. T_{peak} was also included in the state vector x, but its constraints were written alone to make the formulation more readable.

For the case with relaxed constraints 10 temperature points in the grid were used. As the grid had 18 points, this meant that the temperatures at index 0, 2, 4, 6, 8, 10, 12, 14, 16 and 17 were used as inputs, and the rest were found by linear interpolation. The input vector $u_{\text{T,init}}$ was therefore equal to

$$u_{\text{T,init}} = [T_0, T_2, T_4, T_6, T_8, T_{10}, T_{12}, T_{14}, T_{16}, T_{17}] \tag{4.5}$$

The optimization problem was then formulated as in Equation 4.4, except for the constraint on the minimum difference between the inputs. As the points here were closer to each other and the minimum gradient was 10 °C, it was instead formulated as

$$T_i - T_{i-2} \geq 1\,^\circ\text{C} \quad i = [2, 4, ..., 16] \tag{4.6}$$

$$T_{17} - T_{16} \geq 0.5\,^\circ\text{C} \tag{4.7}$$

with the difference between T_{17} and T_{16} being half as much as the others as the points are closer together.

4.3 Optimizing using ram speed

For the optimization using ram speed, the idea was to improve upon the solution that used the initial temperature as input by allowing the ram speed to be manipulated. The optimal initial temperatures from the previous optimization were used as the initial conditions, and only the ram speed was used as an input in the optimization problem. The new formulation thus became:

$$\begin{aligned}
\min_{u_{\text{RamSpeed,t}}} \quad & \sum_{t=0}^{N-1} (T_{\text{peak, t+1}} - T_{\text{peak, sp}})^2 + \rho\epsilon_{t+1} \\
\text{s.t.} \quad & x_{t+1} = g(x_t, u_{\text{RamSpeed, t}}) \\
& c(x_t, u_{\text{RamSpeed, t}}) \leq 0 \\
& x_{min} \leq x_t \leq x_{max} \\
& T_{\text{peak, sp}} - 5\,^\circ\text{C} - \epsilon_t \leq T_{\text{peak, t}} \leq T_{\text{peak, sp}} + 2\,^\circ\text{C} + \epsilon_t \\
& \epsilon_t \geq 0 \\
& u_{\text{RamSpeed, t}} \geq 0 \\
& \Delta u_{\text{RamSpeed, t}} \leq 0.4\,\text{mm/s}^2 \\
& T_{\text{peak, 0}} = 520\,^\circ\text{C}
\end{aligned} \tag{4.8}$$

The difference from the formulation in Equation 4.4 is that the constraints on the initial temperatures have been removed, as these values are fixed, and constraints on the ram speed have been added.

The minimum value allowed for the ram speed is zero, as it is not allowed to move backwards. The maximum acceleration has also been included in the constraint on $\Delta u_{\text{RamSpeed,t}}$. To reduce the complexity of the problem input blocking was performed. The ram speed at the first 15 points in time plus every tenth point beyond that were used as variables, and a first order hold was used to calculate the values in between.

4.4 Optimizing using both initial temperature profile and ram speed

To minimize both deviations in T_{peak} from its set point and the total extrusion time, both the initial temperature profile and ram speed were used as inputs simultaneously. To add the rate of extrusion to the objective function, the deviation of the ram speed from a set point equal to the maximum allowed speed was included in addition to the deviations in T_{peak}. The rest of the optimization problem then becomes a combination of the ones from Sections 4.2 and 4.3:

$$
\begin{aligned}
\min_{u_{\text{T,init}},u_{\text{RamSpeed,t}}} \quad & \sum_{t=0}^{N-1} q_1(T_{\text{peak, t+1}} - T_{\text{peak, sp}})^2 + q_2(u_{\text{RamSpeed, max}} - u_{\text{RamSpeed, t}})^2 + \rho\epsilon_{t+1} \\
\text{s.t.} \quad & x_{t+1} = g(x_t, u_{\text{T, init}}, u_{\text{RamSpeed, t}}) \\
& c(x_t, u_{\text{T, init}}, u_{\text{RamSpeed, t}}) \leq 0 \\
& x_{min} \leq x_t \leq x_{max} \\
& T_{\text{peak, sp}} - 5\,^\circ\text{C} - \epsilon_t \leq T_{\text{peak, t}} \leq T_{\text{peak, sp}} + 2\,^\circ\text{C} + \epsilon_t \\
& \epsilon_t \geq 0 \\
& 0\,^\circ\text{C} \leq u_{\text{T, init}} \leq 660\,^\circ\text{C} \\
& \left(\frac{dT}{dx}\right)_{\text{min}} \leq \frac{du_{\text{T, init}}}{dx} \leq \left(\frac{dT}{dx}\right)_{\text{max}} \\
& 0\,\text{mm/s} \leq u_{\text{RamSpeed, t}} \leq 5\,\text{mm/s} \\
& \Delta u_{\text{RamSpeed, t}} \leq 0.4\,\text{mm/s}^2 \\
& T_{\text{peak, 0}} = 520\,^\circ\text{C}
\end{aligned}
\tag{4.9}
$$

$\left(\frac{dT}{dx}\right)_{\text{min}}$ is either 40 °C/m or 10 °C/m, depending on which of the two temperature constraints are used. $\left(\frac{dT}{dx}\right)_{\text{max}}$ is set equal to 20 °C per point in the grid, which equals approximately 380 °C/m, to have a feasible upper limit to the gradient. An upper limit of 5 mm/s was also added to the ram speed, to keep it inside the feasible operational region. q_1 and q_2 are scalars used to prioritize between the terms in the objective function.

4.5 Software

Below follows a description of the software used in both model implementation and optimization. Software used in this project was developed by Cybernetica [10] for use in model predictive control.

- **Cybernetica Model and Application Component:** Programming template in C, where the model is implemented.
- **Cybernetica CENIT:** Consists of Cenit Kernel and Cenit MMI. Cenit Kernel does the computation related to both optimization and parameter estimation, while Cenit MMI is the user interface.
- **Cenit RealSim:** Simulation tool used to test CENIT by simulating the process to be controlled.

Even though these tools were developed for use in model predictive control [10], it was possible to use them for open loop optimization as well. In model predictive control a prediction of optimal behaviour with a short horizon is made. The response of the system is then measured and the optimization procedure is repeated. Open loop optimization does not have feedback, and instead the optimal behaviour of the whole process is predicted at once.

5 Results and Discussion

The results of the optimizations were compared on two criteria, the extrusion time and the sum of squared deviations of T_{peak} from its set point. As the temperature initially started at 520 °C the deviations were much larger the first 10 s than the rest of the extrusion cycle for all the optimization methods. To better compare the methods the calculation of the sum therefore started after 10 s, so the behaviour after the temperature had time to increase was compared better. The formula used was therefore

$$e = \sum_{t=10}^{N} (T_{\text{peak}} - T_{\text{peak, sp}})^2 \tag{5.1}$$

Exact values for the optimal initial temperatures found are shown in Appendix A. The plots of T_{peak} in Section 5.1, 5.2 and 5.3 are zoomed in around the temperature constraints to better show the behaviour close to the set point. The initial increase in temperature from the starting point of 520 °C is therefore not shown. To be able to compare the optimized results with today's operation, data from an extrusion performed by Hydro is shown below. Figures 5.1 and 5.2 show estimated values for T_{peak} provided by Cybernetica, logged ram speed values from Hydro and the initial temperature profile for the extrusion cycle. This extrusion was not performed at the same ram speed as the optimization, and estimation of T_{peak} was done using a later version of the model than the one used in the optimization. The values of T_{peak} therefore deviate from expected behaviour for the optimization model. Nevertheless, comparing the variations in T_{peak} is still possible.

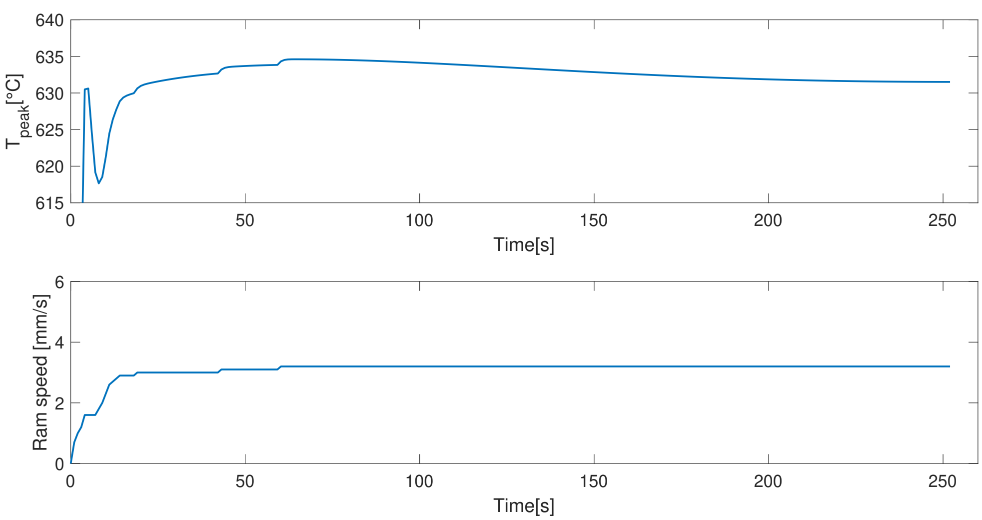

Figure 5.1: Estimated T_{peak} and logged ram speed from an extrusion performed by Hydro.

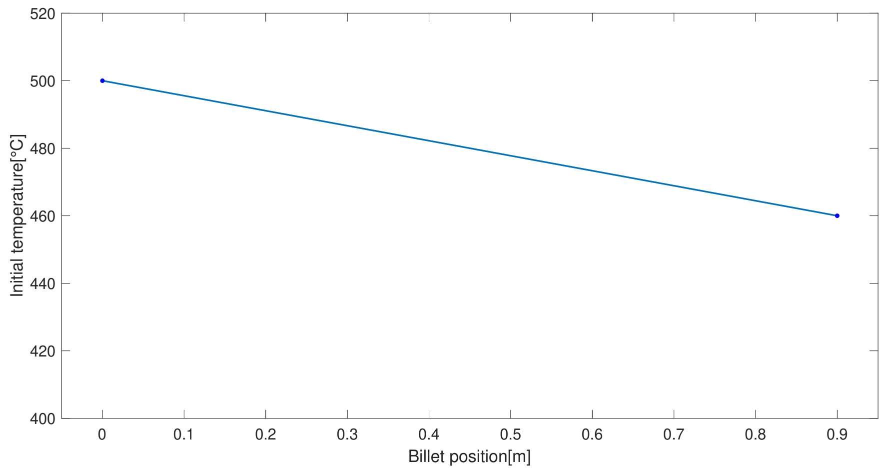

Figure 5.2: Initial temperature profile used by Hydro in an extrusion.

5.1 Optimizing using initial temperature profile

5.1.1 40 °C/m minimum temperature gradient

The results for the case with a minimum temperature gradient of 40 °C/m and a linear profile, only using the initial temperature as input are shown in Figure 5.3. The optimized initial temperature profile is shown in Figure 5.4. The initial temperature difference between the front and back was 36.1 °C. The extrusion time was 220 s and the sum of squared deviations was 1883.502. The results show large deviations in T_{peak}. It reached the upper constrain of $T_{\text{peak, sp}} + 2$ at the start of the extrusion cycle and almost the lower constraint of $T_{\text{peak, sp}} - 5$ later.

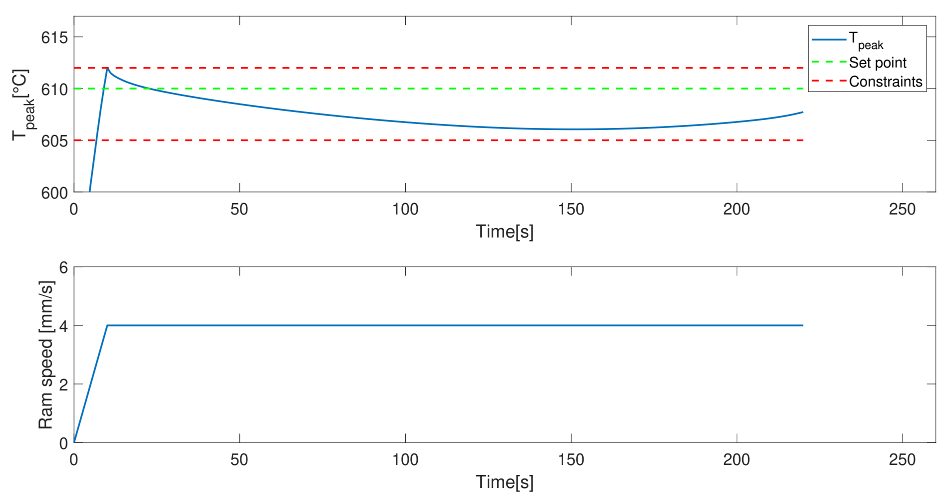

Figure 5.3: Optimal T_{peak} using the initial temperature as the input, with a minimum initial gradient of 40 °C/m. Red lines are constraints and green lines show set points.

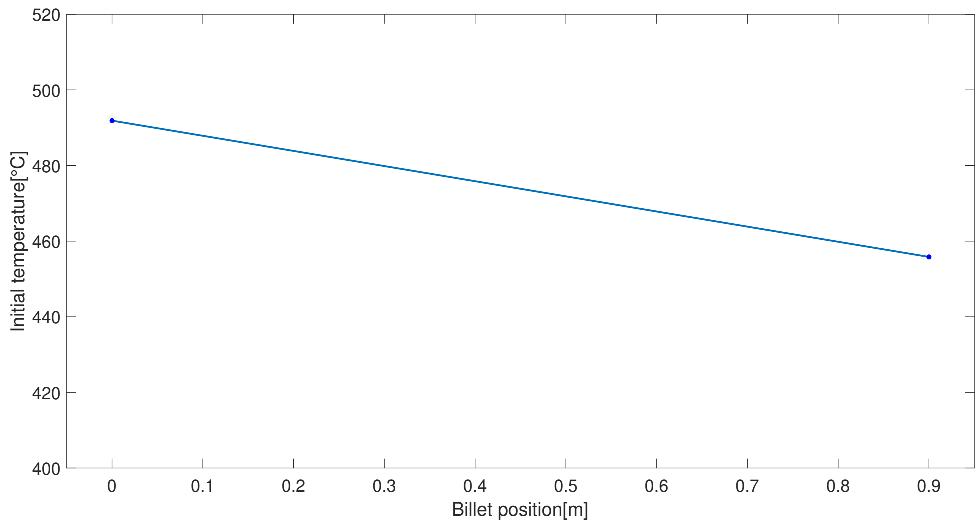

Figure 5.4: Optimal initial temperature profile with a minimum gradient of 40 °C/m.

5.1.2 10 °C/m minimum temperature gradient

The results for the case with a minimum temperature gradient of 10 °C/m and only using the initial temperature as input are shown in Figure 5.5, as well as the fixed profile for the ram speed used in the optimization. The optimized initial temperature profile is shown in Figure 5.6. The extrusion time was 220 s and the sum of squared deviations was 11.231. The results show that T_{peak} was kept quite close to its set point for the entire extrusion cycle after the initial temperature increase from 520 °C. The maximum deviation after this point was approximately 1 °C. Figure 5.6 shows that the optimal initial temperature profile was not linear. For most of the billet the temperature was constrained by the minimum gradient, but at the last two points towards the back part the temperature dropped. The overall temperature difference between the front and back was 39.9 °C.

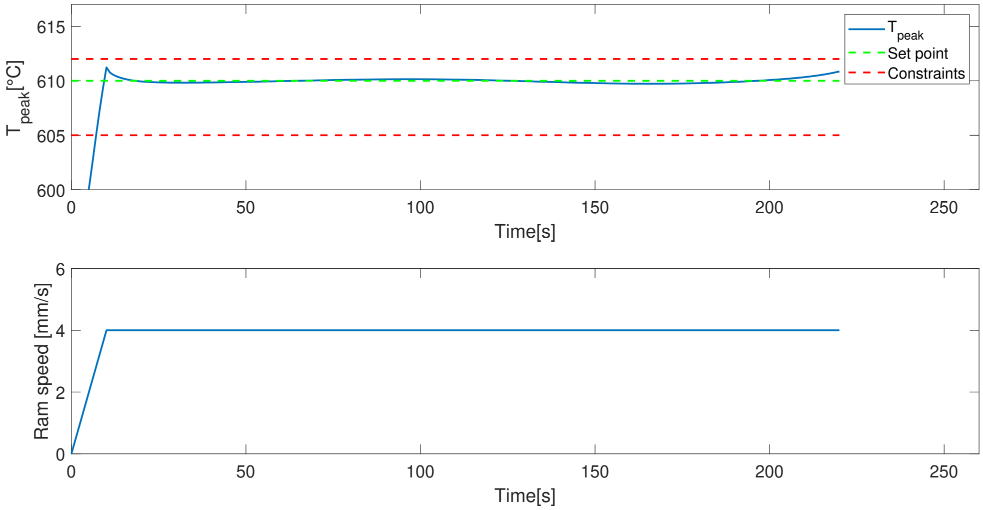

Figure 5.5: Optimal T_{peak} using the initial temperature as the input, with a minimum initial gradient of 10 °C/m. Red lines are constraints and green lines show set points.

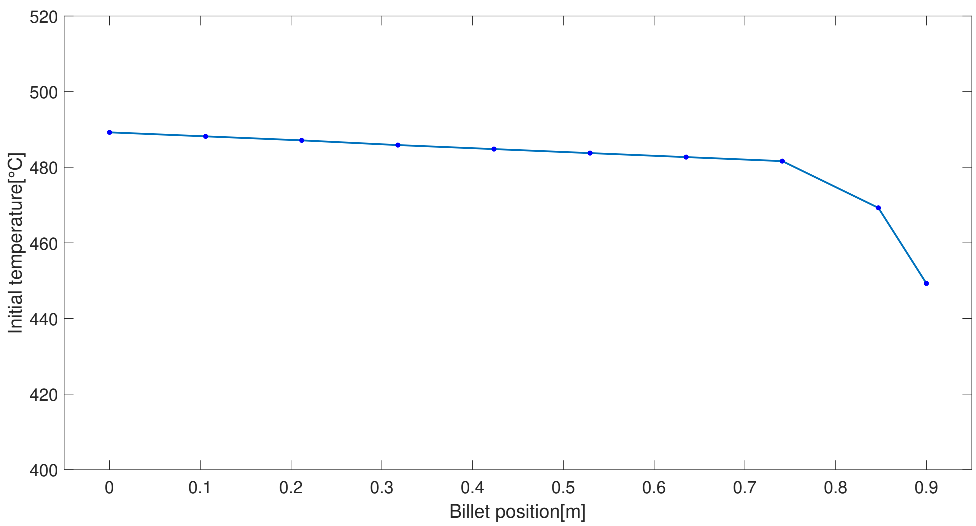

Figure 5.6: Optimal initial temperature profile with a minimum gradient of 10 °C/m.

5.2 Optimizing using ram speed

5.2.1 40 °C/m minimum temperature gradient

The results for the case with a minimum temperature gradient of 40 °C/m and a linear profile are shown in Figure 5.7 and the fixed initial temperature profile is shown in Figure 5.4. The temperatures are the ones calculated in Section 5.1. The extrusion time was 200 s and the sum of squared deviations was 0.004. Optimizing the ram speed removed any significant deviations in T_{peak}. In Figure 5.3 T_{peak} was below its set point for most of the extrusion time, and here this was counteracted with a slowly increasing ram speed until approximately 130 s, after which it slowly decreased again. The increased ram speed also resulted in a 20 s shorter extrusion time.

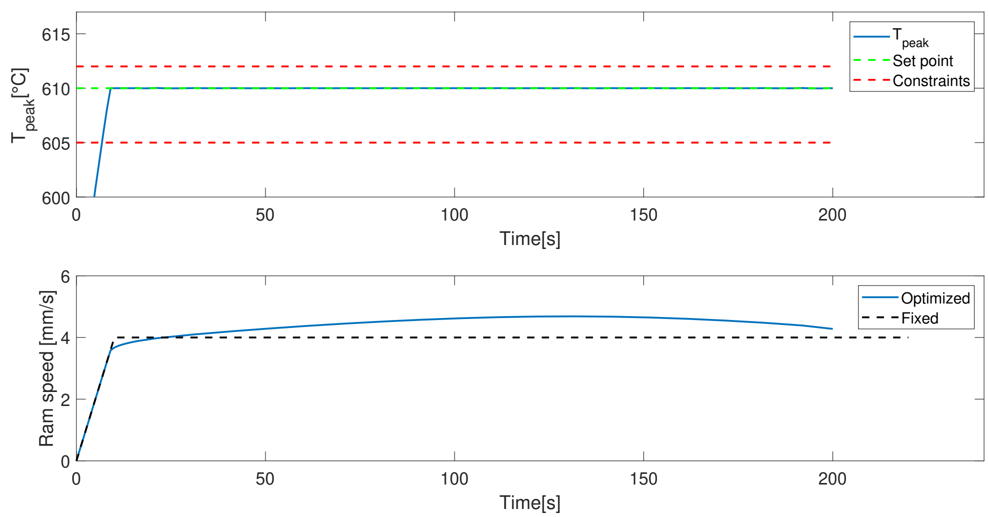

Figure 5.7: Optimal T_{peak} and ram speed using ram speed as the input and using a fixed linear initial temperature profile with a minimum initial gradient of 40 °C/m. Red lines are constraints and green lines show set points. The black dotted line shows the unoptimized ram speed used in Section 5.1.

5.2.2 10 °C/m minimum temperature gradient

The results for the case with a minimum temperature gradient of 10 °C/m are shown in Figure 5.8 and the fixed initial temperature profile is shown in Figure 5.6. The temperatures are the ones calculated in Section 5.1. The extrusion time was 221 s and the sum of squared deviations was 0.489. The optimized ram speed was similar to the fixed profile used in Section 5.1, with some small differences to counteract the deviations in T_{peak} shown in Figure 5.5. The shift from maximum acceleration to stable ram speed was for example more gradual, which removed the initial overshoot in T_{peak} observed at around 10-15 s in Figure 5.5. The ram speed also decreased towards the end of the extrusion, to remove the increase in T_{peak} observed at the end of the extrusion cycle in Figure 5.5. The optimization of the ram speed therefore resulted in only negligible deviations after the initial temperature increase.

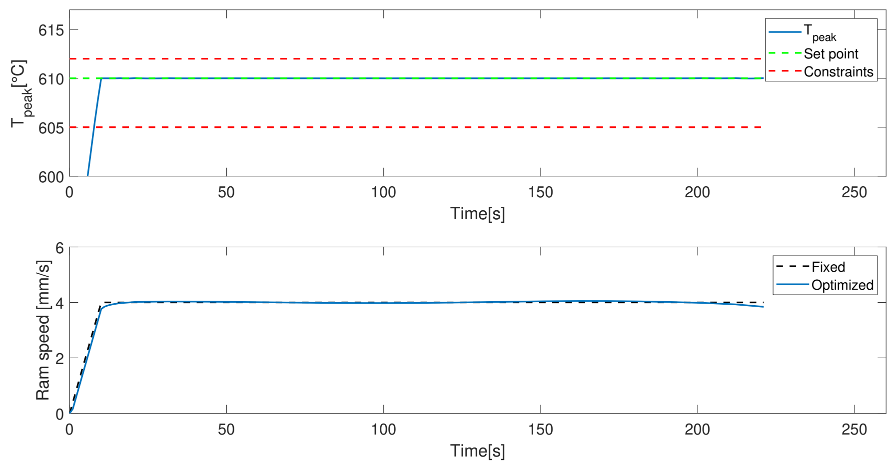

Figure 5.8: Optimal T_{peak} and ram speed using ram speed as the input. The fixed initial temperature had a minimum initial gradient of 10 °C/m. Red lines are constraints and green lines show set points. The black dotted line shows the unoptimized ram speed used in Section 5.1.

5.3 Optimizing using both initial temperature profile and ram speed

5.3.1 40 °C/m minimum temperature gradient

The optimization was tuned to prioritize deviations in T_{peak} over maximizing ram speed for both values of the minimum temperature gradient by setting the value of q_1 to 20 and q_2 to 0.07. These values were found by trial and error. The results for the case with a minimum temperature gradient of 40 °C/m and a linear temperature profile are shown in Figure 5.9 and 5.10. The extrusion time was 200 s and the sum of squared deviations was 0.549. The control of T_{peak} was good, with only a small deviation observed around 150 s, where the ram speed reached its upper limit. This deviation was however small enough to be of limited importance. The temperature difference between the front and back was 57.1 °C.

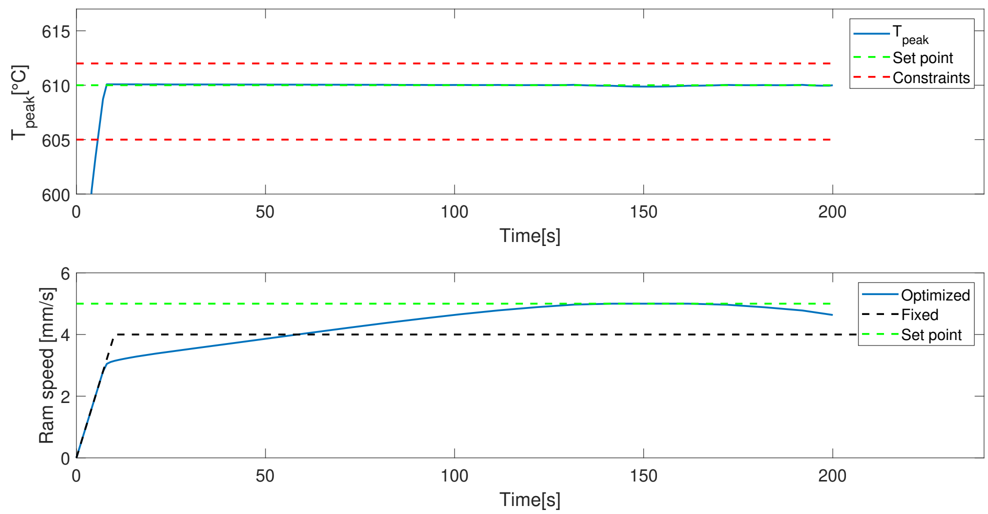

Figure 5.9: Optimal T_{peak} and ram speed using a 2 point temperature profile with a minimum gradient of 40 °C and ram speed as inputs. Red lines are constraints and green lines show set points. For the ram speed plot the green line also marks the upper limit. The black dotted line shows the unoptimized ram speed used in Section 5.1.

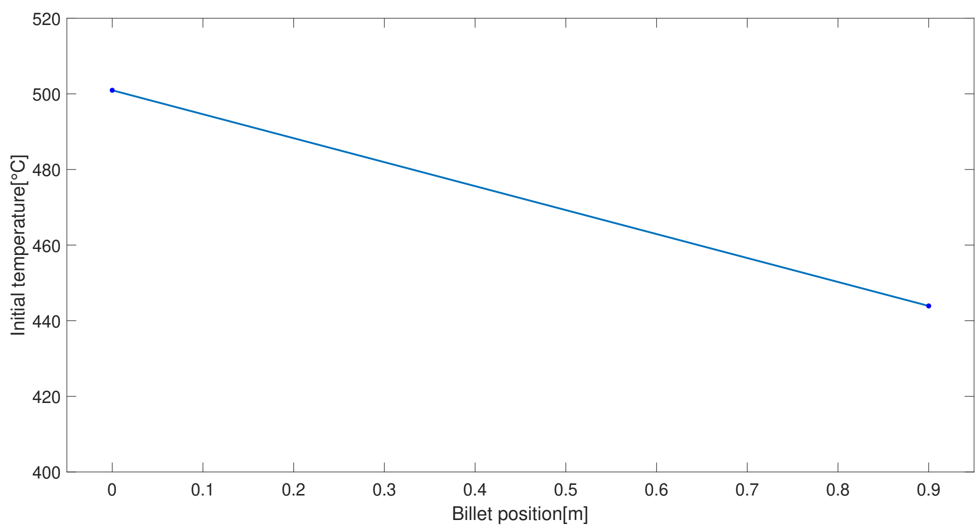

Figure 5.10: Optimal initial temperature profile using a 2 point temperature profile and ram speed as inputs.

5.3.2 10 °C/m minimum temperature gradient

The results for the case with a minimum temperature gradient of 10 °C/m are shown in Figure 5.11 and 5.12. The extrusion time was 187 s and the sum of squared deviations was 0.321. The results show very good control of T_{peak}, with no significant variations in temperature after the initial increase from 520 °C. Some deviations were observed between 20 s and 60 s, but they were too small to be of significance. The ram speed was close to the set point and upper limit of 5 mm/s for most of the extrusion cycle, resulting in a significantly lower extrusion time than when ram speed was the only optimization variable, where the extrusion time for this minimum gradient constraint was 221 s.

Comparing the plots of the ram speeds for the two temperature constraints shows a slower acceleration for the case with a minimum gradient of 40 °C/m, which only reached its upper limit towards the end of the extrusion cycle. The initial temperature profile in Figure 5.12 had an S-shape, with a high gradient close to the front and back and low in the middle. The total temperature difference between the front and the back was 88.2 °C.

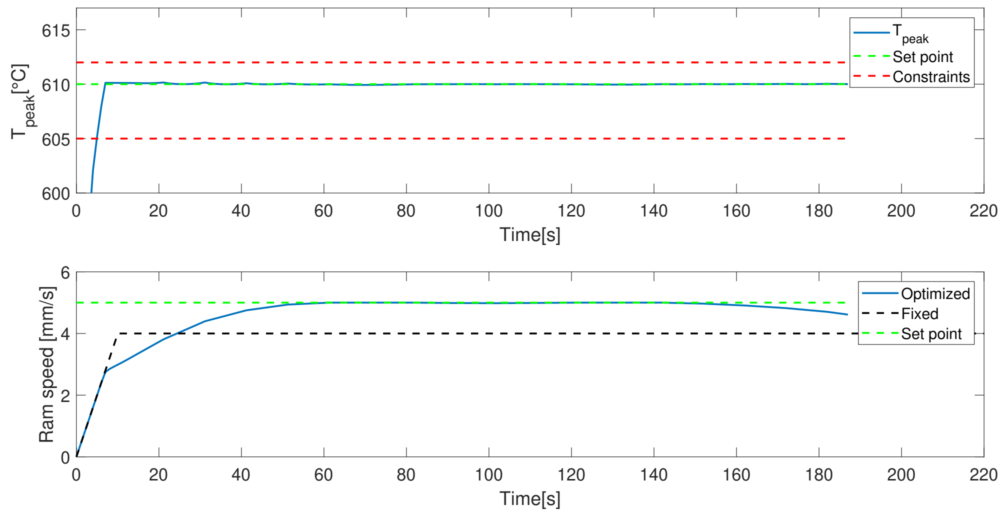

Figure 5.11: Optimal T_{peak} and ram speed using a 10 point temperature profile with a minimum gradient of 10 °C and ram speed as inputs. Red lines are constraints and green lines show set points. For the ram speed plot the green line also marks the upper limit. The black dotted line shows the unoptimized ram speed used in Section 5.1.

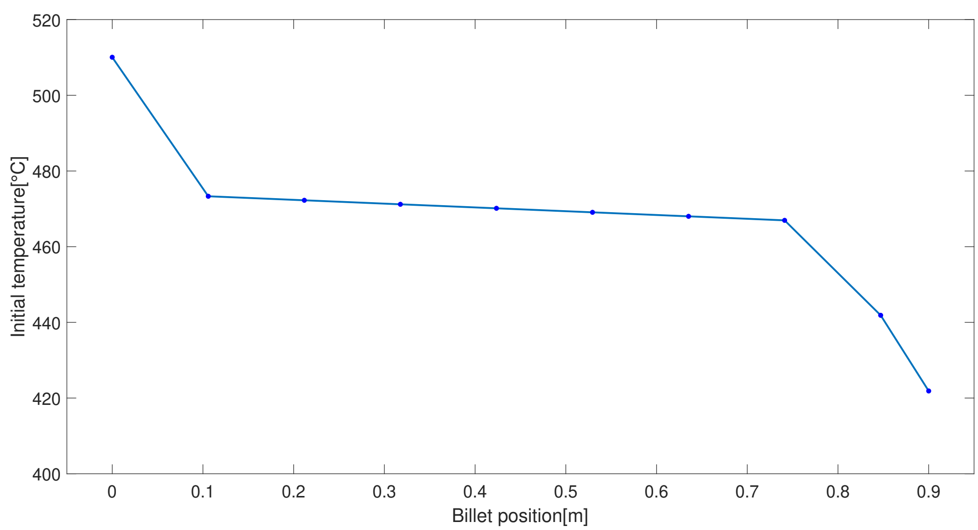

Figure 5.12: Optimal initial temperature profile using a 10 point temperature profile and ram speed as inputs.

5.4 Summary of results

A summary of the results of the optimizations is shown in Table 5.1. It shows that all cases where the ram speed was optimized had low squared temperature deviations, with the lowest being the case where ram speed was optimized for $\left(\frac{dT}{dx}\right)_{\text{min}} = 40\,^{\circ}\text{C/m}$. The shortest extrusion time was achieved for simultaneous optimization of temperature profile and ram speed with $\left(\frac{dT}{dx}\right)_{\text{min}} = 10\,^{\circ}\text{C/m}$.

Table 5.1: Summary of extrusion times and squared temperature deviations (e)

Optimized variable(s)	$\left(\frac{dT}{dx}\right)_{\text{min}}$[°C/m]	Extrusion time [s]	e[°C^2]
Temperature profile	10	220	11.231
Temperature profile	40	220	1883.502
Ram speed	10	221	0.489
Ram speed	40	200	0.004
Both	10	187	0.321
Both	40	200	0.549

5.5 Comparison with data from Hydro

Figures 5.1 and 5.2 show values for T_{peak}, ram speed and the initial temperature profile for an extrusion performed by Hydro. The squared deviations e could not be calculated, as their presses are not operated based on set point tracking for T_{peak}, but instead experience on what gives good product quality. This extrusion was also performed with a lower ram speed than the usual 4 mm/s, so the extrusion time was naturally longer and comparisons with the optimized extrusion times gives little information about possible improvement. It can however still be seen that the variations in T_{peak} were much larger in this extrusion process than in the any of the results from the optimizations. The optimization with fixed ram speed and a linear temperature profile with a minimum initial temperature gradient of 40 °C, with results shown in Figure 5.3, had the worst set point tracking of all the optimization cases. It still had a less than 7 °C difference between the highest and lowest T_{peak} after the initial temperature increase, while the data from Hydro showed a difference of approximately 18 °C. Optimization cases where the ram speed was optimized had a maximum difference of less than 1 °C. This indicated that significant improvements in the control of T_{peak} is possible compared to today's practice.

5.6 Comparison of minimum gradient constraints

Figure 5.12 and 5.10 show the optimized initial temperature profiles for minimum initial temperature gradient constraints of 10 °C/m and 40 °C/m, with a forced linear profile. They show that the lower minimum constraint without forced linearity had much larger temperature differences at the ends of the billet, while being at the minimum constraint in the middle. This allowed a much faster increase in the ram speed shown in Figure 5.11 than for the linear temperature profile, whose ram speed is shown in Figure 5.9. The figures show that after the initial ramp up both ram speeds keep increasing towards the set point of 5 mm/s, but the acceleration was higher for $\left(\frac{dT}{dx}\right)_{\text{min}} = 10\,^{\circ}\text{C/m}$. This was possibly due to the higher initial temperature gradient at the front of the billet. Increased ram speed generates more heat, and thus increases T_{peak}. Therefore, rapid increases in ram speed must be compensated by lower temperature in the billet if T_{peak} is to be kept constant. As the temperature in the front of the billet decreased faster for the nonlinear taper, the ram speed could also be increased faster. This resulted in a 13 s shorter extrusion time for the nonlinear taper. This indicates that the efficiency of the extrusion press could be improved if nonlinear initial temperature profiles are used instead of the linear ones, and the minimum requirement for the temperature gradient is decreased.

For the case where only the initial temperature was optimized, with results shown in Figure 5.5 and 5.3, there was significant difference between the gradient constraints. The nonlinear taper managed much better control of T_{peak} than the linear one, as shown by its much lower squared temperature deviation. Using a nonlinear taper could therefore possibly improve control of T_{peak} for cases with a fixed ram speed as well.

5.7 Comparison of optimization strategies

Two optimization strategies to find the best initial temperature profile and ram speed were used in this project. One first found the optimal temperatures for a fixed ram speed and then optimized the ram speed for this temperature profile to reduce any deviations in T_{peak} still present. This corresponds to first performing the optimization described in Section 4.2 and then the one described in Section 4.3 with the results from the first as the initial temperature. The second strategy optimized both initial temperature and ram speed simultaneously, which corresponds to the optimization problem described in Section 4.4. Here, the rate of extrusion was also included in the objective function, as the problem had more degrees of freedom than before. For the case with a nonlinear initial taper and $\frac{dT}{dx}_{\text{min}} = 10\,°\text{C/m}$ simultaneous optimization resulted in 34 s shorter extrusion time. This low extrusion time was as described in Section 5.6 due to a high initial temperature gradient at the front of the billet allowing high acceleration of the ram. For the linear temperature profile with $\frac{dT}{dx}_{\text{min}} = 40\,°\text{C/m}$, there was however little difference between the optimization strategies. Even though the ram speed profiles were not identical, the total extrusion time was the same. The forced linearity and high minimum gradient therefore seem to have limited the gain from simultaneous optimization.

6 Conclusions

In this project, open loop dynamic optimization of an extrusion process for aluminium was investigated. A first-principle model based on finite differences was used. Set point tracking for the temperature inside the die shaping the extruded profile and minimization of the total extrusion time was implemented using the initial temperature profile of the aluminium billet and the ram speed as manipulated variables. The results discussed in Section 5 showed that very good set point tracking for T_{peak} was achieved. A comparison with data from Hydro indicated that a significant reduction in deviations compared to today's practice is possible. When only the initial temperature was optimized, with a fixed constant ram speed, some deviations in T_{peak} from the set point were observed, but no significant deviations were observed in any of the cases where ram speed was optimized as well. By comparing the Figures 5.3 and 5.7 one can also see that large deviations in T_{peak} were removed with relatively small changes in ram speed. As the heater used to generate the initial taper for the billet only has 4 induction points for a billet this size, it is uncertain how well the optimal tapers can be reproduced in a real system. It is therefore important to note that even if these exact profiles cannot be reproduced, good control of T_{peak} should still be possible to achieve by optimizing ram speed.

Significant reduction of the extrusion time was also achieved through optimization of the ram speed, compared to using a fixed speed of 4 mm/s. For the case with a linear taper and minimum initial temperature gradient of 40 °C/m a reduction of 20 s was achieved while still managing good set point tracking for T_{peak}. For the nonlinear taper with minimum initial temperature gradient equal to 10 °C/m the reduction was 34 s. This indicates that significant improvement of the efficiency of the extrusion presses is possible, even for the linear initial taper constraint practised today. Even higher efficiency could however be achieved by improving control of the initial temperature profile, to allow for nonlinear tapers. In conclusion, dynamic optimization of the extrusion process showed high potential for improving operation, and should be investigated further.

The model used in the optimizations was still in development when this project was undertaken, and the values of the calculated optimal temperatures and ram speeds are therefore not expected to accurately describe the optimal conditions for the real system. This project should therefore not be considered to have found the optimal way to extrude aluminium. It instead indicates that dynamic optimization of extrusion of aluminium has a high potential for improving both product quality and efficiency when model development is complete.

7 Recommendations for further work

As the work in this project was done as part of a course corresponding to half the work load for a single semester, there are several important factors that could not be investigated due to the limited time available. These are described below, along with suggested actions to be taken.

As described in Section 6, it is uncertain how well some of the optimal initial temperature profiles can be reproduced in the actual system, due to limited precision in the heater used to pre-warm the billet. Cybernetica has models for both the heater and the transition from heater to extrusion press, and to get a better understanding of the behaviour of the system as a whole, these models should also be included in the optimization. This way one could find optimal temperatures more likely to be realizable in practice.

The extrusion presses in this project have cooling available in the die, but this degree of freedom was not utilized in the optimization. Including it could possibly allow for more rapid extrusion, as it would be able to counteract the temperature increase caused by higher ram speed. One possible option could be to run the press at max ram speed during the whole extrusion process, and use the cooling for set point tracking for T_{peak}.

Rough estimates for some constraints in the process were used in the optimization, as accurate values were not available. The maximum allowed ram speed of 5 mm/s was set to keep the behaviour of the press inside the assumed feasible region of operation, but a value based on test of the extrusion press should be found to improve the optimization. The minimum gradient constraints on the initial temperature of the billet were also not based on empirical trials. For the linear profile the minimum constraint was the value used in practice by Hydro, but as better temperature control is developed for the process this value might change. For the nonlinear temperature profile, the value of the minimum gradient was not based on any common practice or tests, as no tests with nonlinear gradients have been performed. It was set to a quarter of the minimum gradient for the linear profile, so the differences between the constraint could be illustrated.

The process model used in the optimization was still under development when this project was undertaken. Therefore, more accurate estimated values could be found by reoptimizing when the model is finished. This should be done before drawing any more conclusions from the results.

To ensure good operation of the extrusion presses, feedback control should also be implemented. This could be done by implementing nonlinear model predictive control, with the goal of following the optimal trajectories calculated in the open loop dynamic optimization. This way, disturbances and model mismatch could be accounted for. There are then several options for practical implementation of the open loop optimization for the extrusion press. It could be performed before every extrusion, to calculate optimal behaviour for each individual billet. It could also be used to calculate optimal behaviour for each product, and these results could be stored until needed. This would mean less strict requirements on the computation time for the optimization. If optimization is to be performed for each billet, it has to take less time than an extrusion cycle. Optimization cases in this project took up to three minutes to perform, and the computational time is expected to increase if the heaters and cooling are included. Therefore, model simplifications might be necessary if optimization for each billet is desired.

References

[1] Aukrust, T., and LaZghab, S. Thin shear boundary layers in flow of hot aluminium. *International Journal of Plasticity 16* (2000).

[2] Bastani, A. F., Aukrust, T., and Brandal, S. Study of isothermal extrusion of aluminum using finite element simulations. *Springer-Verlag France* (2010).

[3] Bastani, A. F., Aukrust, T., and Brandal, S. Optimisation of flow balance and isothermal extrusion of aluminium using finite-element simulations. *Journal of Materials Processing Technology* (2011).

[4] Bird, R. B., Stewart, W. E., and Lightfoot, E. N. *Transport phenomena*, 2nd ed. John Wiley & Sons, 2006.

[5] Foss, B., and Heirung, T. A. N. Merging optimization and control. *Technical report* (2016).

[6] Jakobsen, H. A. *Chemical Reactor Modeling*, 1st ed. Springer, 2008.

[7] Matamoros, C. F. C. Modeling and control for the isothermal extrusion of aluminium. *Swiss Federal Institute of Technology Zurich* (1999).

[8] Nocedal, J., and Wright, S. J. *Numerical Optimization*, 2nd ed. Springer, 2006.

[9] Pedersen, B. aluminium. `https://snl.no/aluminium`. Accessed on 10.10.2021.

[10] Cybernetica. Technology model predictive control. `https://cybernetica.no/technology/model-predictive-control/`. Accessed on 23.11.2021.

[11] Encyclopedia of Mathematics. Finite-difference calculus. `https://encyclopediaofmath.org/index.php?title=Finite-difference_calculus`. Accessed on 22.11.2021.

[12] Hydro. Micro-channel tubes. `https://www.hydro.com/en/aluminium/products/precision-tubes/micro-channel-tubes/`. Accessed on 02.12.2021.

[13] Scholarpedia. Stiff systems. `http://www.scholarpedia.org/article/Stiff_systems`. Accessed on 22.11.2021.

[14] The Research Council of Norway. Extrutec - high precision extrusion temperature control through digital technology. `https://prosjektbanken.forskningsradet.no/en/project/FORISS/313919?Kilde=FORISS&distribution=Ar&chart=bar&calcType=funding&Sprak=no&sortBy=date&sortOrder=desc&resultCount=30&offset=120&TemaEmne.2=IKT-n%C3%A6ringen`. Accessed on 10.10.2021.

A Optimized Initial Temperatures

Table A.1 and A.2 show the optimized initial temperatures from the optimization problems described in Section 4.2 and 4.4, for both values of the minimum allowed gradient. The values in Table A.1 were also used as the initial condition in the optimization problem described in Section 4.3.

Table A.1: Optimal initial temperatures from the optimization using only these as inputs. All temperatures are in degrees Celsius.

	$\left(\frac{dT}{dx}\right)_{\text{min}} = 10\,°\text{C/m}$	$\left(\frac{dT}{dx}\right)_{\text{min}} = 40\,°\text{C/m}$
T_0	489.2	491.9
T_2	488.2	487.6
T_4	487.1	483.4
T_6	485.9	479.2
T_8	484.8	474.9
T_{10}	483.7	470.7
T_{12}	482.7	466.4
T_{14}	481.6	462.2
T_{16}	469.3	458.0
T_{17}	449.3	455.8

Table A.2: Optimal initial temperatures from the optimization using initial temperature and ramspeed as inputs. All temperatures are in degrees Celsius.

	$\left(\frac{dT}{dx}\right)_{\text{min}} = 10\,°\text{C/m}$	$\left(\frac{dT}{dx}\right)_{\text{min}} = 40\,°\text{C/m}$
T_0	510.1	501.0
T_2	473.3	494.2
T_4	472.3	487.5
T_6	471.2	480.8
T_8	470.1	474.1
T_{10}	469.1	467.4
T_{12}	468.0	460.6
T_{14}	467.0	453.9
T_{16}	441.9	447.2
T_{17}	421.9	443.9